

# Conductivity in ferroelectric transition

R. BACSEI<sup>a</sup>, C. MINDRU<sup>a</sup>, C.-P. GANEA<sup>b</sup>, H. V. ALEXANDRU<sup>a,c\*</sup>

<sup>a</sup>*Faculty of Physics, University of Bucharest, Romania*

<sup>b</sup>*National Institute of Materials Physics, Bucharest-Magurele, Romania*

<sup>c</sup>*Academy of Romanian Scientists, 54 Splaiul Independentei, RO-050094, Bucharest, Romania*

Triglycine sulphate crystal (TGS) is one of the most studied ferroelectric materials, having a second order transition around 49 °C. The complex dielectric constant we have measured on the frequency range 1 Hz – 10 MHz and on a large temperature range, in para and in ferroelectric phase. Conductivity was estimated based on the Grant (J. Appl. Phys 1958) model. Literature data, (Rajesh et al, Materials Letters 2002) shall be used to estimate conductivity activation energy of four TGS doped crystals. Experimental and calculated data shall be discussed.

(Received September 2, 2013; accepted November 7, 2013)

**Keywords:** Ferroelectrics, TGS crystal, Conductivity, Activation energy

## 1. Introduction

TGS single crystal has found important applications in electronic, as pyroelectric detectors [1], ferroelectric data storage devices, nanofabrication, candidates for nonvolatile memories, etc. Several studies were focused on the lattice dynamics [2-3], dielectric relaxation [4, 5] and relaxation of ferroelectric domain wall [6-8]. Single crystal structure [9] and ferroelectric parameters [10] were reported. We have earlier presented [11-13] the kinetic, the growth conditions and several important characteristic of pure and doped TGS crystals. Two fundamental relaxation mechanisms and a “hybrid” one, we have analyzed in recent presentations [14-18].

## 2. Experimental

Single crystal growth, sample preparation and measurements procedures were mainly presented

in refs. [14, 15]. In short, crystals were grown by slow solvent evaporation at 54 °C, i.e. in paraelectric phase. Usually, crystals grown bellow the Curie point get mechanical tensions at the limit of antiparallel domain boundaries, which in turn always decreases electrical properties.

Alpha-A Novocontrol dielectric spectrometer and Sample Cell ZGS, were used on the frequency range 1÷10<sup>7</sup> Hz for measurements. Temperature was monitored from room temperature to 65 °C, were for 30 min it was kept constant and then down at a pace of 0.6 °C/min. Both component of permittivity were automatically registered and analyzed [16÷18]. Conductivity of the TGS sample shall be analyzed and compared with some literature data [19, 20]. We shall reconsider and analyze the experimental data from ref [21].

## 3. Results

The frequency dependence of the two components of permittivity [22], further used, is:

$$\varepsilon' = \varepsilon_{\infty} + \frac{(\varepsilon_{st} - \varepsilon_{\infty})}{1 + \omega^2 \tau_{\varepsilon}^2} \quad (1)$$

$$\varepsilon'' = \frac{\omega \tau_{\varepsilon} (\varepsilon_{st} - \varepsilon_{\infty})}{1 + \omega^2 \tau_{\varepsilon}^2} + \frac{\sigma}{\varepsilon_0 \omega} \quad (2)$$

where  $\varepsilon_{st}$  and  $\varepsilon_{\infty}$  are the extreme values of the real component of permittivity in the Cole-Cole representation [22],  $\tau_{\varepsilon}$  is the relaxation time and  $\sigma$ -conductivity. In eq. (2) the first term represent the dielectric losses and the second one the conduction losses.

The frequency dependence of experimental data corresponding to the imaginary component of permittivity at 43 °C is presented in Fig.1. Data have been decomposed in two terms and fitted vs. frequency. In this figure the peak value of the three components of permittivity is slightly displaced and depressed when the conductivity component “c” is subtracted. This component “c” exceeds 90% from the measured permittivity at 1 Hz, represent 28% at 1 kHz and about 8 % at 1 MHz. In fig.1, at the peak values of the imaginary component of permittivity  $\varepsilon''$ , approximately at 10<sup>2</sup> Hz, 10<sup>4</sup> Hz and 3.510<sup>5</sup> Hz, the “c” component represent 26% 20% and 8% respectively. These component values changes with temperature as discussed in ref [14].

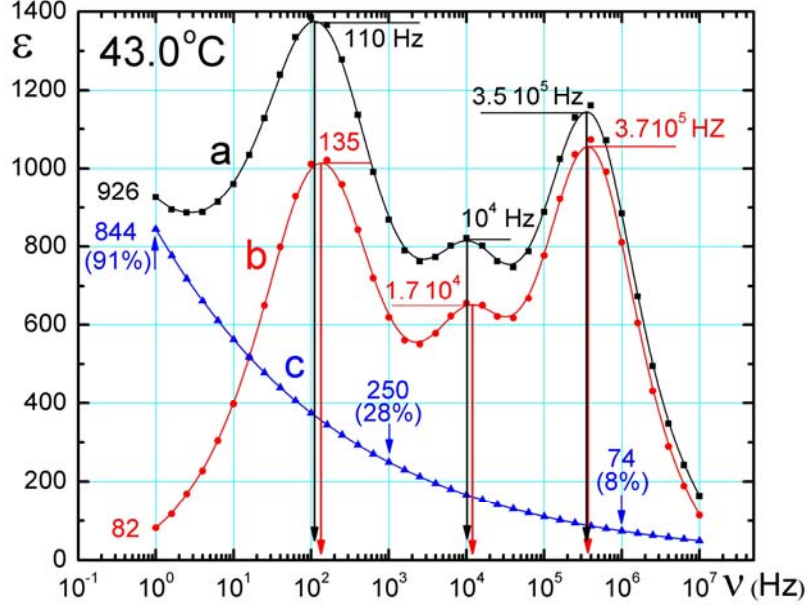


Fig.1. The decomposition of the imaginary component  $\epsilon''$  of the dielectric constant. The measured curve "a" was decomposed according to eq. (2) in the dielectric losses curve "b" and the conduction losses curve "c" respectively.

The low frequency component of  $\epsilon''$  in fig.1, represents the ferroelectric domains dynamic with a typical relaxation time  $\tau_L \sim 10^3$  sec and Arrhenius temperature dependence, i.e. an activation energy of about 0.7 eV ( $\sim 28$  K<sub>B</sub>T) [14, 16]. The higher frequency component in the MHz range, (called in the literature "the critical slowing down" mechanism), represents a molecular relaxation mechanism ( $\tau_H \sim 10^{-7}$  sec), characteristic to the ferroelectric transition with a long distance order in the lattice and weak temperature dependence. The middle frequency contribution around 10<sup>4</sup> Hz in the temperature range 35 °C  $\div$  T<sub>C</sub> seems to be the interaction of higher frequency component with the lattice dynamic [14].

#### 4. Conductivity estimation

The two components of conductivity were estimated using the Grant [23] mechanism:

$$\sigma' = \omega \epsilon_o \epsilon'' \quad (3)$$

$$\sigma'' = \omega \epsilon_o (\epsilon' - \epsilon_\infty) \quad (4)$$

where  $\epsilon_o = 1/36 \pi 10^9$  F/m and theirs frequency dependence is presented in fig. 2. In this figure both components change the slope around 1 kHz and 1 MHz according to the relaxation time previously mentioned (see also ref [14]).

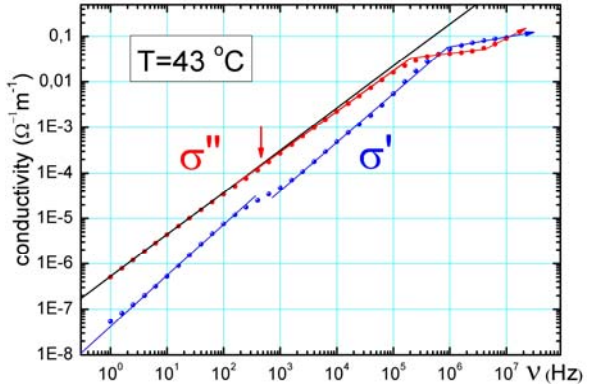


Fig.2. The two component of conductivity vs. frequency in double log scale. The constants in equations (3) and (4) on two frequency ranges are given in table I.

Table 1. Constants in the analytical representation of the two components of conductivity in equations (5) and (6) on two frequency ranges (fig. 2).

$\sigma'' (\Omega^{-1} m^{-1}) = a v^b$				$\sigma' (\Omega^{-1} m^{-1}) = c v^d$			
1 – 10 <sup>3</sup> Hz		10 <sup>3</sup> – 10 <sup>5</sup> Hz		1 – 10 <sup>3</sup> Hz		10 <sup>3</sup> – 10 <sup>6</sup> Hz	
a	b	a'	b'	c	d	c'	d'
5.1 <sub>6</sub> 10 <sup>-7</sup>	0.91 <sub>6</sub>	7.7 <sub>6</sub> 10 <sup>-7</sup>	0.88 <sub>3</sub>	4.2 <sub>4</sub> 10 <sup>-8</sup>	1.1 <sub>2</sub>	1.9 10 <sup>-8</sup>	1.09 <sub>5</sub>

In Fig.2 on several frequency ranges the curves support the analytical representation (see table 1) of the type:

$$\sigma'' = a v^b \quad (5)$$

$$\sigma' = c v^d \quad (6)$$

There is a visible slope change of both conductivity components around  $v \sim 1$  kHz and  $\sim 1$  MHz. The slope of  $\sigma''$  in Fig.2 decreases from 0.91<sub>6</sub> to 0.88<sub>3</sub>, (i.e. ~4%) around 10<sup>3</sup> Hz and from 1.1<sub>2</sub> to 1.09<sub>5</sub> (i.e. ~2%) around 1 MHz (see also ref. [15]).

Under this form, the conductivities vs. frequency, in double log scale cannot offer more details.

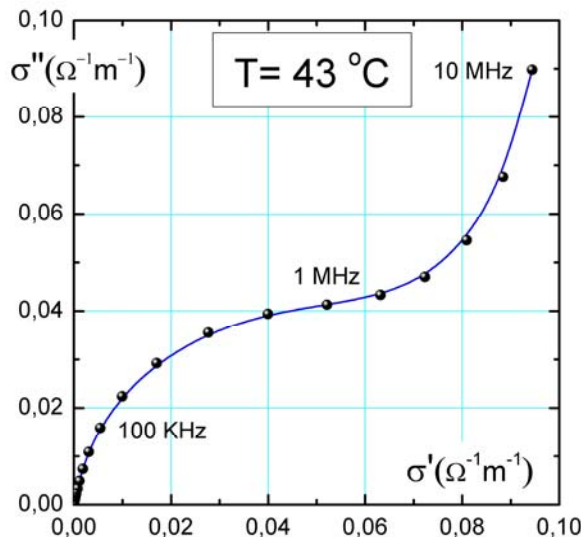


Fig.3. The Grant [23] representation of the conductivity components  $\sigma''$  vs.  $\sigma'$ . These couple of parameters was represented for five selected frequencies every frequency decade.

In fig. 3 we present ( $\sigma''$  vs.  $\sigma'$ ) data according to Grant representation [23], at 43 °C. This is a typical representation, but the three frequency zone, as in Cole-Cole (fig. 1) representation [14, 15] cannot be discerned. However, the extrapolation of this representation toward the lower frequencies, as in Fig. 4, allows estimating

$\sigma_o = 2.5 \cdot 10^{-9} \Omega^{-1} m^{-1}$  the DC conductivity. This figure agrees with some other literature data [24]. Particularly, at 1 Hz the conductivity component of  $\varepsilon''$  (i.e. the second term in eq.2) represent more than 90 % from the experimentally measured value (see fig. 1).

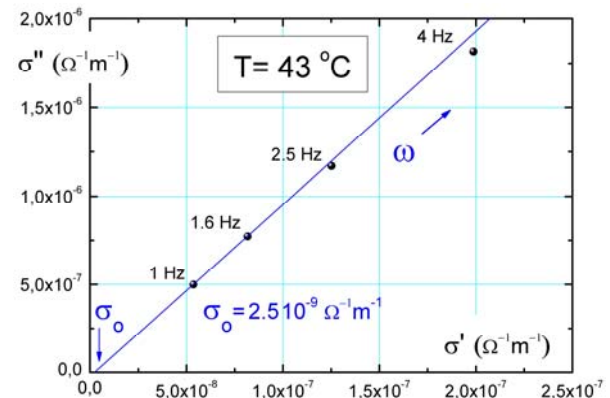


Fig. 4. Data from fig.3 extrapolated to the lowest measured frequency allows estimating  $\sigma_o$  - the DC conductivity.

## 5. Literature data

The conductivity of TGS doped samples was measured in ref. [21]. Here, the TGSP basic substance analyzed was obtained by partially substitution of phosphate with sulphate (no percent substitution mentioned). The other three analyzed samples were TGSP doped with amino acids having similar structure to glycine: ATGSP (L-aniline TGSP), VTGSP (L-Valine GSP) and asp-TGSP (L-asparagine TGSP).

As mentioned in the original paper [21], the conductivity was measured on c-cut samples, i.e. not on ferroelectric “b” section and the temperature dependence was estimated according to equation:

$$\sigma = \sigma_o \exp \left[ -\frac{Ea}{k_B T} \right] \quad (7)$$

The activation energies  $Ea$  estimated by the authors [21] are presented in table 2, first row, only on the temperature interval 30–60 °C.

Table 2. Activation Energy  $E_a$  (eV) estimated on several temperature intervals for TGS impurified samples using data from ref. [21]. The notations a, b, c, d corresponds to the samples from fig.5.

Temperature (°C)	Activation Energy $E_a$ (eV)			
	TGSP (a)	asp-TGSP (b)	V-TGSP (c)	A-TGSP (d)
30-60 Ref [21] ⇒	0.025	0.073	0.051 <sub>5</sub>	0.089
30-50	0.04	0.05	0.056	0.062
60-100	0.16	0.32	0.28	0.26
100-140	0.67	0.92	0.96	0.90

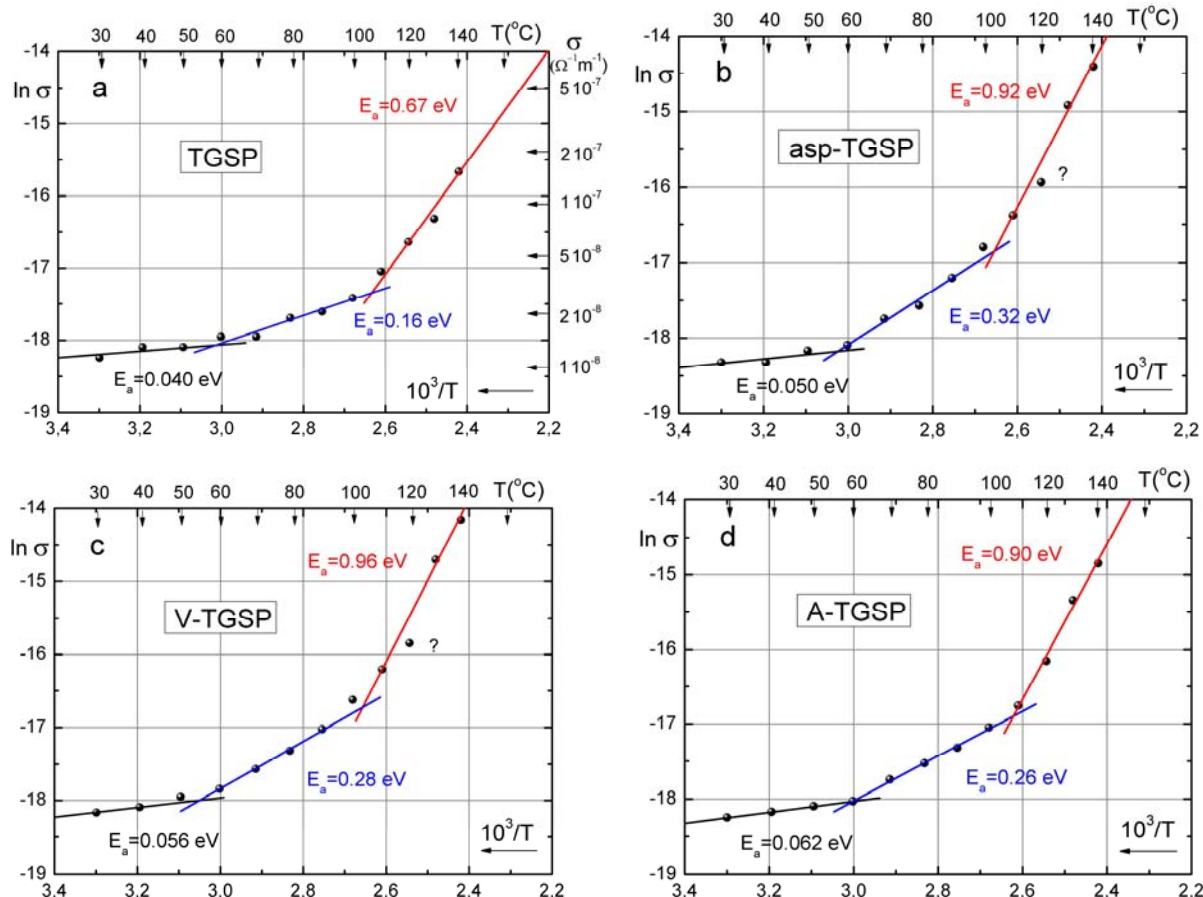


Fig. 5. Arrhenius representation of conductivity for the TGS impurified crystals, estimated using the original data from ref. [21]. Lower abscissa scale  $10^3/T$  was reversed. The upper abscissa (nonlinear) scale shows increasing temperature in Celsius degree.

We have drawn carefully the experimental data from fig. 1, ref [21] and we have built the Arrhenius temperature dependence of the four crystals as in Fig. 5 (no such analyze was presented in the original paper). We have considered “ $\sigma 10^8$  mho” (! ?) in the ordinate of Fig. 1, ref. [21], to be international system conductivity units.

There are clearly three temperature intervals having several activation energies, see Table 2.

## 6. Discussions

We shall further analyze data presented in ref [21]. Measurements were made on a large temperature range 30-140 °C and “the observations” (quotation from [21]), where made while cooling the sample (probably measurements were made, not observations). In Fig. 5 the Arrhenius representations of the conductivity

corresponding to several doped samples shows three distinct regions of the temperature dependence. However, it is not clear if DC, 1 kHz, or other type of conductivity was measured in the original paper [21].

On this temperature range there is a slope break between 50-60 °C and another one around 100-110 °C.

In the low temperature region 30-60 °C, where graphic accuracy representation of the data in fig 1 of the ref. paper [21] is low, the activation energy, we have

*Table 3. Conductivity and activation energy Ea (eV) estimated using data from refs. [19], [20], [21] and the present data.*

Crystal	TGS [19]	TGS [20]	NBSTGS (20 mol%), [20]	TGSP [21]	TGS present data	
$\sigma_{DC} (10^{-11} \Omega^{-1} m^{-1})$ T = 35 °C	0.1	5.5	16.2	1300	~250 T = 43 °C	~2 T = 65 °C
Ea (eV) (ferro Phase)	1.7	1.4 <sub>2</sub>	1.2 <sub>5</sub>	0.025 (?)	---	---
Ea (eV) (para Phase)	0.7	0.71	0.42	0.67 T > 100 °C	---	---

The absolute value of the conductivity around 35 °C (ferro phase) in the ref. [21] - see also the data in fig. 5, are two to four order of magnitude higher than in the literature [19], [20]. Our present estimated data at 43 °C are still one order of magnitude higher (line one in table 3).

At higher temperatures 100-140 °C the activation energy of conductivity 0.67±0.96 eV we have found (Fig.5 and the fourth line in table 2) is close to some other literature data [19, 20] in paraelectric phase, but at somewhat lower temperatures (line three in table 3).

In the table 2 (line three) the activation energy on 60÷100 °C temperature range, we have estimated from the graphics in fig.5. The activation energy values on this temperature range do not comply with the literature data. In the para phase we have found the activation energy Ea = 0.67 eV, for TGSP at T > 100 °C, which is close to 0.7 eV found in refs. [19], [20] (table 3) at lower temperatures (50 ÷ 80) °C. This suggest that the surface conduction due to the water vapors adsorbed on the lateral sample surfaces between the two electrodes is essential in the (60 ÷ 100) °C temperature range [21]. Indeed, for TGSP activation energy Ea = 0.16 eV in table 2, line 2, is substantially smaller than 0.7 eV found in refs. [19], [20].

In the paraelectric phase at 65 °C we have estimated for pure TGS the value  $\sigma_{DC} \approx 2 \cdot 10^{-11} \Omega^{-1} m^{-1}$  (line one in Table 3) in good agreement with some literature data [19].

The slope change in the Arrhenius representations (Fig. 5), around the transition point is quite normal, but the slope change around 100 °C might suggest the surface conductivity has an important contribution in the measurements performed in ref [21] at lower temperatures.

In ref. [19] the conductivity measurements were made under the humidity atmosphere control and the activation energy Ea estimated in ferro and in para phase particularly, are quite similar to the data found in ref. [20] (see the two columns [20] in the table 3).

estimated (0.04 ÷ 0.06) eV, (see fig.5) is not far from the figures estimated in the original paper (first and second lines in table 2). However, the figures are much too low versus other literature data estimated on the ferroelectric region (see the second line in table 3). This might be due to the measurements made in ref. [21] on the section "c" of the samples, not in ferroelectric section, or to some other causes.

In the ferro phase, indeed the activation energy Ea = 0.025 eV, ref. [21] (or 0.04 eV we have found, table 2), for TGSP is about two order of magnitude lower than the literature data [19], [20] (table 3) suggesting the surface conductivity has indeed the essential role.

The conductivity of our pure TGS sample we have estimated from measurements performed in the nitrogen stream (the normal working regime of Alpha-A Novocontrol dielectric spectrometer). The value we have found  $\sigma \approx 2.5 \cdot 10^{-9} \Omega^{-1} m^{-1}$ , at 43 °C which is still about two orders of magnitude higher than other literature data (line one in table 3) suggest the conductivity in the ferro phase is extremely sensitive to the surface conduction (ionic crystals as TGS are sensitive to water moisture). The conductivity  $\sigma \approx 1.3 \cdot 10^{-8} \Omega^{-1} m^{-1}$  we have estimated at 35 °C from ref. [21] (see fig. 5) is even one order of magnitude higher than our measurements and confirm this assertion.

The conductivity and the complex impedance of KDP ionic crystal grown in solutions of several pH (2.35-4.82) was measured on the frequency range 100 Hz ÷ 1 MHz in ref. [24]. Thus, measurements were made in the para phase from room temperature to ~140 °C. The conductivity of the samples prepared even from the same single crystal differ by several order of magnitude, i.e. from ~4·10<sup>-9</sup> to 4·10<sup>-5</sup>  $\Omega^{-1} m^{-1}$  and the "activation enthalpy" was found in the range 0.5-0.7÷0.9 eV. Impurities Fe<sup>3+</sup> and Al<sup>3+</sup>, which involve the defects structure and the proton non-stoichiometric concentration in crystals grown in solutions of several pH were found responsible for such variations.

Our pure TGS sample has higher conductivity ( $10^{-5} \div 10^{-1} \Omega^{-1} m^{-1}$ ) in fig. 2 than KDP crystals from ref. [24], on the same frequency range. It might be supposed the conduction mechanism in TGS is similar to the ionic KDP crystals, based on impurity and proton hoping mechanism, having appropriate activation energy of conduction in para phase (approx. 0.7 eV – line three in Table 3).

## 7. Conclusions

Dielectric spectroscopy of the TGS measured crystal was used on the frequency range 1 Hz ÷ 10 MHz. The measured dielectric components have been used to find the conductivity components, using Grant [23] procedure. The frequency analytical dependence of the conductivity components was found on the mentioned frequency range (table 1).

The DC component of conductivity (of about  $10^{-9} \Omega^{-1} m^{-1}$ ) was fairly estimated at 43 °C, as an example, by extrapolation of ( $\sigma''$  vs.  $\sigma'$ ) representation towards lower frequencies.

The experimental data of a set of four TGS impurified samples, from ref. [21], have been used to find the activation energy of conductivity on several temperature ranges (table 2). Data have been compared with some other literature data (table 3).

Activation energy of the samples considered in ref. [21], we have carefully analyzed, agree with some other literature data only for temperatures higher than 100 °C. This suggests that on the middle temperature range 60÷100 °C in para phase and 30÷50 °C in ferroelectric phase, the surface conductivity has a dominant contribution.

In the ferroelectric range of TGS, the measured conductivity can be essentially affected (several orders of magnitude) by the surface conductivity if the samples are not protected against water moisture adsorbed from the atmosphere. This effect can affect the electrical parameters of electronic devices, using unprotected TGS pure or doped samples.

## Acknowledgements

This paper was supported by the sectorial operational program human resources development (sop HRD), financed from the European social fund and by the Romanian government under the contract number sop HRD/107/1.5/s/82514.

## References

- [1] S. B. Lang, D.K. Das-Gupta, Ferroelectrics Rev **2**, 266 (2000).
- [2] Genowefa Słosarek, A Heuerf, H Zimmermannf, U Haeberlent, J. Phys.: Condens. Matter **1**, 5931 (1989).
- [3] Andrew P Giddy, Martin T Dove, Volker Heinei, J. Phys.: Condens. Matter **1**, 8327 (1989).
- [4] G. Luther, Phys. Stat. Sol. (a) **20**, 227 (1973).
- [5] K. Kuramoto, H. Motegi, E. Nakamura, K. Kosaki, J. Physical Society Japan, **55**, 377 (1986).
- [6] J. Fousek, V. Janousek, Phys. Stat. Sol. **13**, 195 (1966).
- [7] J. Zhang, Phys. Stat. Sol. (a) **193**, 347 (2002).
- [8] J. Zhang, Ferroelectrics, **281**, 105 (2002).
- [9] S. Hoshino, Y. Okaya, R. Pepinsky, Phys. Rev. **115**, 323 (1959).
- [10] S. Hoshino, T. Mitsui, F. Jona, R. Pepinsky, Phys. Rev. **107**, 323 (1957).
- [11] H.V. Alexandru, C. Berbecaru, Cryst. Res. Technol. **30**, 307 (1995).
- [12] H.V. Alexandru, C. Berbecaru, Mater. Sci. Semicond. Process. **5**, 159 (2003).
- [13] H. V. Alexandru, Annals New York Academy of Sciences **1161**, 387 (2009).
- [14] C. Mîndru, C. P. Ganea, H. V. Alexandru, J. Optoelectron. Adv. Materials **14**, 157 (2012).
- [15] H.V. Alexandru, C. Mîndru, C. Berbecaru, Digest J. Nanomater. Biostructures, **7**, 2141 (2012).
- [16] Horia V.Alexandru, Carmen Mîndru, C. Paul Ganea, Florin Stănculescu, Stefan Antohe, "Metastable State and Relaxation in Ferroelectric Transition of Pure TGS Crystals", Invited Lecture in International Conference **ROCAM 2012**, Aug. 28-31 Brasov, Romania.
- [17] Horia V. Alexandru, Carmen Mandru, Constantin Paul Ganea, Raluca Bacsei, "Mechanism of relaxation and characteristic time in ferroelectric TGS crystals" Plenary Lecture in Intern. Conference **BRAMAT 2013**, Brasov, Feb.28 – March 02, 2013
- [18] Horia V. Alexandru, Carmen Mîndru, Constantin-Paul Ganea, Liviu Nedelcu, "Dielectric spectroscopy in ferroelectric relaxation of TGS crystal", Invited Lecture in **IBWAP 2013** (Internat. Balkan Workshop Applied Physics), Constanta.
- [19] F. Moravek, J.Novotny, J. Phys Soc. Japan **24**, 787 (1968).
- [20] Chitharanjan Rai, K.Byrappa, S.M.Dharmaprakash, Physica B, **406**, 3308 (2011).
- [21] N.P. Rajesh, C. Mahadevan, P. Santhana et al, Materials Letters, **55**, 394 (2002).
- [22] K.S. Cole, R.H. Cole, J. Chem. Physics, **9**, 341 (1941).
- [23] F. A. Grant, J. Appl. Physics **29**, 76 (1958).
- [24] E. D. Yakushkin, E. P. Efremova, A. I. Baranov, Crystallography Reports **46**, 830 (2001). Translated from Kristallografiya, **46**(5), 904 (2001).

\*Corresponding author: horia@infim.ro